Journal of Magnetism and Magnetic Materials 436 (2017) 85–90

Contents lists available at ScienceDirect

Journal of Magnetism and Magnetic Materials

journal homepage: www.elsevier.com/locate/jmmm

Research articles

Tunable magnetocaloric effect around room temperature by Fe doping in $Mn_{0.98}Cr_{(0.02-x)}Fe_xAs$ compound

Jhon J. Ipus [a], Paula O. Ribeiro [b], P. von Ranke [b], R.J. Caraballo Vivas [c], Alexandre M.G. Carvalho [d], Adelino A. Coelho [e], Victorino Franco [a], Daniel L. Rocco [c,f,*]

[a] Department of Condensed Matter Physics, ICMSE-CSIC, Sevilla University, P.O. Box 1065, 41080 Sevilla, Spain
[b] Instituto de Física Armando Dias Tavares, Universidade do Estadodo Rio de Janeiro – UERJ, Rua São Francisco Xavier, 524, 20550-013 RJ, Brazil
[c] Instituto de Física, Universidade Federal Fluminense, Av. Gal. Milton Tavares de Souza s/n, 24210-346 Niterói, RJ, Brazil
[d] Laboratório Nacional de Luz Síncrotron, CNPEM, 13083-970 Campinas, SP, Brazil
[e] Instituto de Física Gleb Wataghin, Universidade Estadual de Campinas – UNICAMP, Caixa Postal 6165, 13083-970 Campinas, S. Paulo, Brazil
[f] Departamento de Formação Geral, Centro Federal de Educação Tecnológica de Minas Gerais – CEFET-MG, Campus Timóteo, 35.180-008 MG, Brazil

ARTICLE INFO

Article history:
Received 28 November 2016
Received in revised form 31 March 2017
Accepted 14 April 2017
Available online 18 April 2017

Keywords:
Magnetocaloric effect
MnAs and derivatives
Magnetic entropy change
Composite

ABSTRACT

In this work, we present an investigation of the magnetic and magnetocaloric properties of $Mn_{0.98}Cr_{(0.02-x)}Fe_xAs$ compounds with x = 0.002, 0.005 and 0.010. Our findings show that as Fe content increases the unit cell volume decreases, which indicates that Fe doping emulates the pressure effect on the crystalline structure. The transition temperature T_C decreases as x increases and it can be set at approximate value of room temperature by changing the doping level. In addition, the magnetic entropy change ΔS_M was determined using a discontinuous measurement protocol, and realistic values from the magnetocaloric effect presented by MnAs-type compounds under pressure (emulated pressure) could be obtained. The values of ΔS_M^{MAX} are very large, around -11 J kg^{-1} K^{-1} with ΔH = 15 kOe, which is higher than that observed for most compounds with T_C around room temperature. However, ΔS_M is confined to a narrow temperature range of 11 K. To overcome this drawback, the composition of a theoretical composite formed by our samples was calculated in order to obtain a table-shaped ΔS_M curve. The simulated composite showed a high value of full width at half maximum δT_{FWHM} of 33 K, which is much higher than that of single sample.

1. Introduction

The magnetocaloric effect (MCE) is the basis of magnetic refrigeration, which is considered an environment-friendly technology because it uses no CFC or HCFC gases, besides being noiseless and energetically efficient. The MCE corresponds to the reversible heating and cooling of conventional magnetic materials when they are placed in a magnetic field and removed from it, respectively. The MCE can be expressed either in terms of an adiabatic temperature change ΔT_{ad} or in terms of an entropy change ΔS when the magnetic field is applied in isothermal conditions.

MnAs-type compounds have been intensively studied in recent years due to the high values of the MCE, which can lead to their use in magnetic refrigeration working at temperatures near room temperature [1,2] when their hysteresis are eliminated. The intense MCE is associated with magnetic transition, which is coupled to structural transition from hexagonal NiAs-type ($T < T_C \sim 300$ K) to orthorhombic MnP-type ($T_C \sim 300$ K $< T$) structure. In fact, the compound suffers another structural transition from orthorhombic to hexagonal at $T_t = 398$ K [3]. At temperatures above T_t, the material is paramagnetic following the Curie–Weiss law, whereas at temperatures between T_C and T_t the material is also considered paramagnetic but it fails in following the Curie–Weiss law [4,5]. In fact, some theoretical studies using density functional [6] and first principles calculations [7] have shown that between T_C and T_t the material exhibits a short-range antiferromagnetic interaction confined to the *ab* plane. This result was recently confirmed by an experimental work[5].

The magnetic and magnetocaloric properties of MnAs and their derivatives are extremely dependent on structural deformation, and therefore, a few kbars of applied hydrostatic pressure can significantly change the magnetic properties. Along with hydrostatic pressure, chemical doping can also generate a structural deformation and emulate the pressure effect. In some cases the two

* Corresponding author at: Instituto de Física, Universidade Federal Fluminense, Av. Gal. Milton Tavares de Souza s/n, 24210-346 Niterói, RJ, Brazil.
E-mail address: rocco@if.uff.br (D.L. Rocco).

http://dx.doi.org/10.1016/j.jmmm.2017.04.030
0304-8853/

approaches are equivalent [5]. Chemical doping can be achieved by replacing Mn or As with other elements. It is important to address that the substitution with Mn is more commonly used to change the magnetic properties compared with the substitution with As, as seen in literature where Mn is replaced by other transition metals [8,9]. In one case, when the Mn was replaced with Fe [1] and Cr [10] a considerable increase in MCE and reduction of thermal hysteresis, respectively, were reported. However, the large MCE values presented by $Mn_{1-x}Fe_xAs$ compounds were overestimated because the MCE depends on the magnetic and thermal history of the system and the hysteresis of the phase transformation is the feature that generates the irreversibility effects. These effects led to overestimation of ΔS_M values when using isothermal magnetization curves for obtaining the MCE response. Thus, it is well known in the magnetocaloric community that for materials exhibiting first-order magnetic transition it is necessary to adopt some measurement protocol for obtaining the isothermals (M vs H curves) in order to calculate realistic MCE values [11,12], or use isofield curves [13].

In this work, we use chemical doping to emulate the pressure effect and study its effect on the magnetic and magnetocaloric properties of the $Mn_{0.98}Cr_{(0.02-x)}Fe_xAs$ compounds. Our main goal is to obtain realistic values of the MCE exhibited by MnAs and their derivatives under hydrostatic pressure since they were recently overestimated [1,2]. Therefore, a discontinuous measurement protocol [11] was used to avoid miscalculating MCE values, and it was applied to samples with different Fe/Cr doping level, i.e., with different emulated pressures. In addition, the compressibility value of MnAs was used to estimate the equivalent relative hydrostatic pressure, which ranges from 0–0.5 kbar (considering x = 0.002 as 0 kbar), and matched the pressure values used in early works [1,2]. Finally, in order to obtain a table-shaped ΔS_M curve, the composition of a composite produced with the three samples was determined, and the ΔS_M curve with a full width at half maximum (δT_{FWHM}) of 33 K was found.

2. Experimental techniques

A previous work [10] has shown that the Cr-doped MnAs compound exhibits a reduced thermal hysteresis, when comparing with pure MnAs compound. On the other hand, the Fe-doped MnAs seem to exhibit the MCE and hysteresis enhanced [1]. Thus, we made a co-doping using the Cr and Fe in order to obtain a compound with optimized properties, namely, a MCE enhanced and hysteresis reduced. Thus, we prepared samples of the $Mn_{0.98}Cr_{(0.02-x)}Fe_xAs$ compound with x = 0.002, 0.005 and 0.010. The samples were prepared following the route presented before [1,14]. The X-ray diffraction at 300 K and Rietveld refinement were used in order to verify if the samples are single phase and to determine the cell parameters. Magnetic properties were studied using a Lakeshore 7407 vibrating sample magnetometer with a maximum applied magnetic field of 1.5 T. The ramping rate at which the M(T) curves were obtained was the same for all samples, around 0.25 K/s. The shape (cubes of ~1 mm of length per side) and mass (around 1.5 mg) of the samples used during the magnetic measurements also were comparable in all cases.

3. X-ray diffraction

X-ray diffraction patterns at room temperature were analyzed by the Rietveld method, which shows that the samples are single phase and crystallize in the orthorhombic phase for the samples with x = 0.005 and 0.010. Fig. 1 shows that the sample with x = 0.002 exhibits peaks of two phases (hexagonal and orthorhombic) because of the phase coexistence observed in the hysteresis

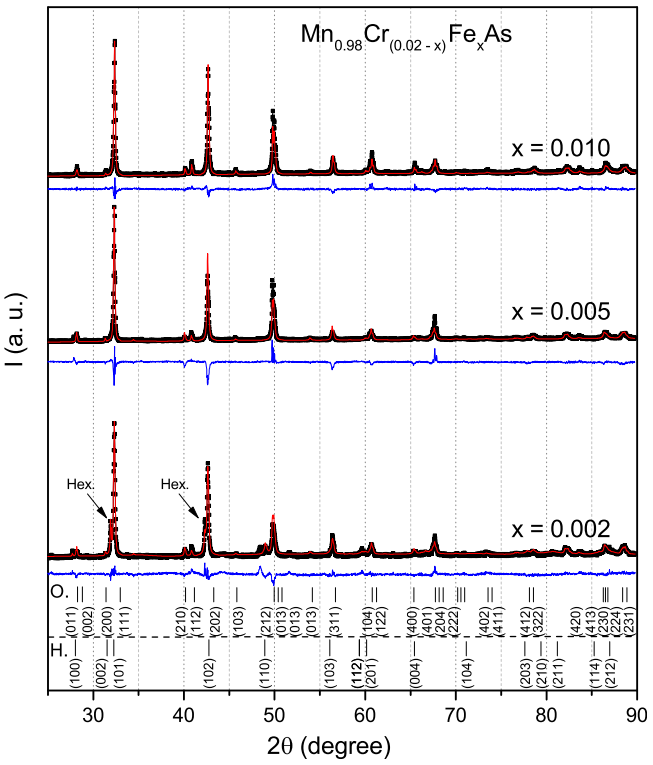

Fig. 1. X-ray diffraction patterns with the correspondent Rietveld refinement for all samples at room temperature. In the bottom is shown the Bragg reflections with the corresponding indices of crystallographic plane for the orthorhombic and hexagonal phases. Note that the sample with x = 0.002 shows the peaks of the hexagonal and orthorhombic phases coexisting at that temperature. The main peaks of the hexagonal phase are indicated by arrow.

region [4,15]. Rietveld fitting shows 86(1)% of orthorhombic phase and 14.3(6)% of hexagonal one for the sample with x = 0.002 at 300 K. The refinement parameters are presented in Table 1 (only for the orthorhombic phase), which shows that the lattice parameters decrease as Fe amount increases, as shown in Fig. 2-Top. The resulting effect on the crystalline structure are better visualized in Fig. 2-Bottom, which shows the unit cell volume as a function of the Fe atoms, which decreases with x. This is expected because the average ionic radius of Fe is lower than that of Cr. Previous works on the Mn_xFe_xAs system showed a similar tendency. Note that the Fe doping emulates the positive pressure effect. From the compressibility of MnAs [5], the corresponding hydrostatic pressure could be determined. Considering x = 0.002 as P = 0 kbar, the values for samples with x = 0.005 and 0.010 are 0.3 and 0.5 kbar, respectively, as seen in Fig. 2-Bottom.

Table 1
Refined crystallographic data and reliability factors for the $Mn_{0.98}Cr_{(0.02-x)}Fe_xAs$ samples in the orthorhombic phase.

Parameters	Samples		
x (Fe amount)	0.002	0.005	0.010
a (Å)	5.7062(3)	5.7026(3)	5.7015(3)
b (Å)	3.6499(3)	3.6478(2)	3.6467(2)
c (Å)	6.3487(5)	6.3467(3)	6.3455(3)
Volume (Å^3)	132.22(2)	132.03(2)	131.93(2)
R_p (%)	3.8	5.7	4.8
R_{wp} (%)	5.1	8.8	6.6
R_{exp}(%)	3.1	3.4	3.3
χ	1.6	2.6	2.0

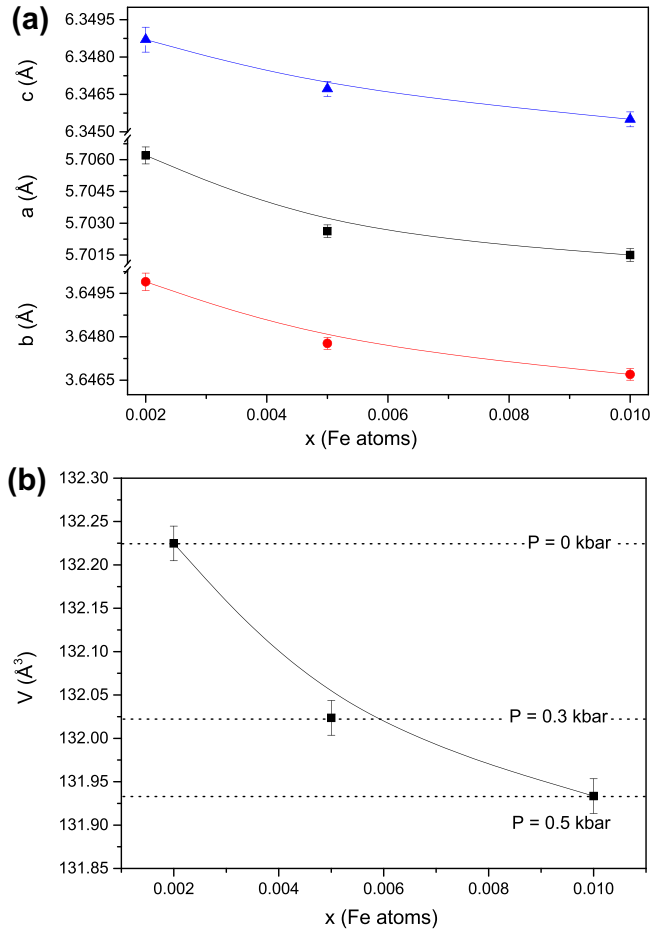

Fig. 2. (Top) Lattice parameters of the orthorhombic phase as a function of the Fe atoms for all studied samples. (Bottom) Unit cell volume as a function of x. Note that the volume decreases as Fe atoms increase. Lines are a guide to the eye.

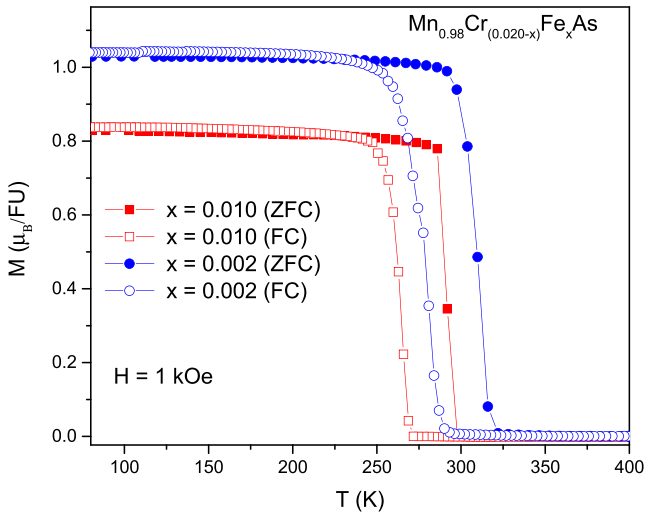

Fig. 3. Magnetization as a function of temperature with applied magnetic field of 1 kOe for two studied samples. For the sake of clearness we are showing only the curves of two samples.

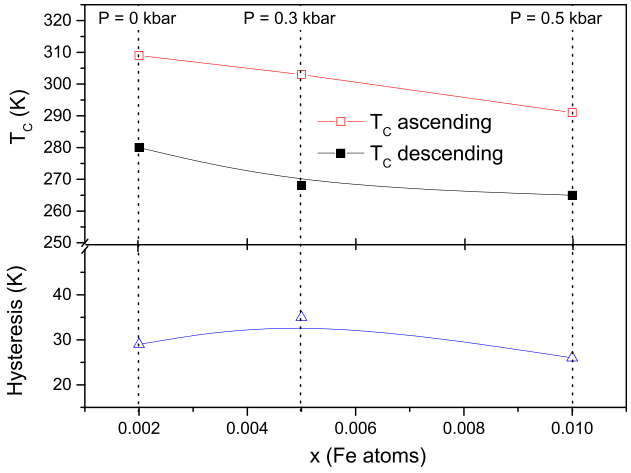

Fig. 4. Top – Curie temperature and (bottom) hysteresis dependencies of the Fe amount with magnetic field applied of 1 kOe. The equivalent hydrostatic pressure was estimated using the unit cell volume and compressibility of MnAs. Lines are a guide to the eye.

4. Magnetic properties and magnetocaloric effect

The structural modification exhibited by the compound when Cr is replaced with Fe should modify the magnetic properties as well. In order to verify this relation, the curves of magnetization as a function of temperature in a magnetic field of 1 kOe were obtained. Fig. 3 shows the curves of magnetization of the x = 0.002 and 0.010 compounds, and it is observed that the T_C decreases as the Fe amount increases. The transition temperature T_C was defined as the minimum in the dM/dT vs T curves, and its dependence on x can be better visualized in Fig. 4 in the heating and cooling regimes. The lower unit cell volume decreased the transition temperature, which is consistent with observations of previous works [5]. This transition temperature dependence on volume, can be ascribed to the itinerant (band) magnetism nature. When the volume decreases, the bandwidth energy increases so the density of states at the Fermi level decreases destroying the magnetic order, as expected from the Stoner criterion. This behaviour is identical to the result of MnAs compound subjected to hydrostatic pressure, and it has already been demonstrated that the two approaches are equivalents in low doping regime [5]. The corresponding hydrostatic pressures calculated before are shown in Fig. 4. By using those results, it is possible to find the displacement of T_C for lower temperatures, which occurs at a rate of −31 K/kbar for increasing temperature and −34 K/kbar for decreasing temperature. This is larger than the displacement of temperature observed for other derivatives of MnAs [5]. Thus, the magnetic properties of the Fe,Cr co-doped MnAs seems to be more sensitive to pressure effect than other members of its family. For comparison, in $Gd_5Si_2Ge_2$ the measured rates were 3.8 K/kbar and 3.2 K/kbar for cooling and heating precesses[16], respectively.

Besides, it is interesting to note that all compounds exhibit a transition around room temperature, which varies with the Fe amount. The magnetic transitions are very close to each other, so that a composite produced with these three samples can extend the temperature range of the maximum ΔS_M values.

Fig. 3 also shows the existence of a thermal hysteresis of 30 K, which is a consequence of the first-order magnetic phase transition coupled to structural transformation from the hexagonal (T < T_C) to orthorhombic phase (T > T_C).

4.1. Magnetocaloric effect

The magnetic data presented in the previous section demonstrated that all samples show a first-order magnetic phase transition. Thus, the calculation of ΔS_M using Maxwell's relations must

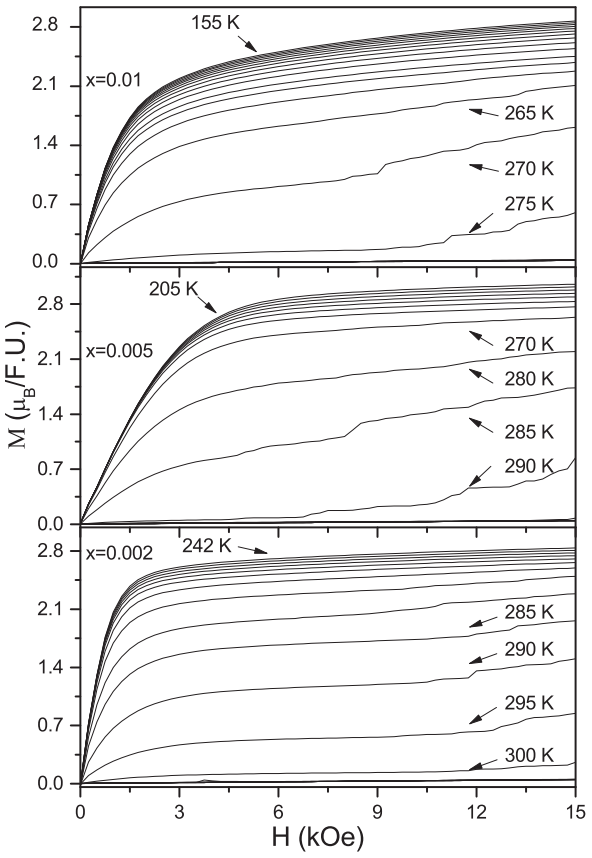

Fig. 5. Isothermals used to obtain the ΔS_M curves for all samples. They were obtained with a temperature increment of 5 k around T_C and of 10 K for the other intervals. The temperature of the last isothermal is 385 K for all samples. Still, a discontinuous cooling protocol [11] was used to ensure each isothermal to start from an uniform magnetic state and so to avoid overestimated ΔS_M values.

be performed such that realistic values are obtained. For this propose, we can use either constant field measurements as a function of temperature, or isothermal measurements as a function of field. However, in this latter case, it is necessary to prepare the sample in a properly defined state that eliminates the coexistence of phases [12]. This can be performed for the current sample either by heating up the sample in zero field well above the transition in between isothermal measurements and using the magnetization curve (from 0 to H_{max}) [12] or also by cooling down in a large enough field down to a temperature well below the transition temperature and using the demagnetization curve (from H_{max} to 0) [11]. The software used for the measurements [17] uses this "discontinuous" or "loop" protocol. In the present work, the isothermal magnetization curves were measured according to a discontinuous measurement protocol [11,12] where each isotherm was obtained by heating the sample well above the transition temperature (paramagnetic state) and cooling it back to the measurement temperature (cooling protocol). This protocol provided the response of the material after all thermal and magnetic history had been erased; therefore, unrealistically high values of MCE were avoided. Thus, ΔS_M was calculated by processing the temperature and field dependent magnetization curves (Fig. 5) using a numerical approach to the expression:

$$\Delta S_M = \mu_0 \int_{H_1}^{H_2} \left(\frac{\partial M}{\partial T}\right)_H dH, \quad (1)$$

where M is the magnetization and T the temperature and H_1 and H_2 are the minimum and maximum applied fields. The partial derivatives are replaced by finite differences and the integration is performed numerically. This procedure was performed with the help of the Magnetocaloric Effect Analysis Program [17].

ΔS_M of all samples are shown in Fig. 6 for a magnetic field variation from zero to 15 kOe, which can be produced by a permanent magnet. The values of ΔS_M for the samples are very high compared to that of most known compounds with T_C at temperatures near room temperature. Table 2 shows ΔS_M^{Max} values for compounds that exhibit T_C of approximately 300 K, and it is evident that the compounds studied in the present work show larger values of ΔS_M. In this case, the values are not overestimated because we used an appropriate measurement protocol. However, as seen in Table 2, our samples show high values of relative cooling power (RCP), but the δT_{FWHM} is not very high[18]. In order to overcome this drawback, we used the ΔS_M values from Fig. 6 and simulated the composition of a composite that could be produced from our samples in order to obtain a table-shaped ΔS_M.

4.2. Composite

As indicated before, the studied compounds present a very high ΔS_M^{MAX} in a very low temperature interval close to T_C of the samples. Thus, in order to overcome this drawback, an optimum composite material formed by the $Mn_{0.98}Cr_{(0.020-x)}Fe_xAs$ series with x = 0.002, 0.005 and 0.010 was calculated. The optimum profile for ΔS_M *vs.* T, to be considered, for example, in an Ericsson cycle, should present: 1) large temperature interval δT_{FWHM} with considerable ΔS_M and 2) ΔS_M values as constant as possible (table-like profile) in the δT_{FWHM} range[26]. The second condition is required for the regenerative

Table 2
Maximum magnetic entropy change ($-\Delta S_{MAX}$) for $\Delta H = 15kOe$, full width at half maximum (δT_{FWHM}) and relative cooling power (RCP = $-\Delta S_M^{max} * \delta T_{FWHM}$) for our samples of the $Mn_{0.98}Cr_{(0.020-x)}Fe_xAs$ system and other important materials on magnetic refrigeration context. For future comparison purpose we present the RC values, which is calculated by using the integral of ΔS_M (T).

Compound	T_C (K)	ΔH (kOe)	$-\Delta S_M^{MAX}$ (J/kg K)	δT_{FWHM} (K)	RCP/RC (J/kg)	Ref.
x = 0.002	**280**[1]	**15**	**7.6**	**18**	**138/157**[2]	**This work**
x = 0.005	**268**[1]	**15**	**11.3**	**11**	**124/150**[2]	**This work**
x = 0.010	**265**[1]	**15**	**10.3**	**11**	**113/133**[2]	**This work**
$La(Fe_{0.92}Co_{0.008})_{11.9}Si_{1.1}$	301	20	8.7			[19]
$PrMn_{1.4}Fe_{0.6}Ge_2$	25.5	15	8.2			[20]
$Gd_5Si_2Ge_2$	276	20	6.5	**16**	**104**	[21]
$Sm_{0.6}Sr_{0.4}MnO_3$	126	15	7.2	16	115	[22]
$Ni_{46}Mn_{43}Sn_{11}$	288	18	7.9	3.8	30.2	[23]
$MnFeP_{0.63}Ge_{0.12}Si_{0.25}$	300	15	11			[24]
$Fe_{88}Zr_7B_4Cu_1$	295	15	1.32	125	166	[25]
Simulated Composite	–	**15**	**4.7**	**33**	**155/163**[2]	**This work**

[1] T_C takes on cooling.
[2] RC = $\int_{T_1}^{T_2} \Delta S_M dT$.

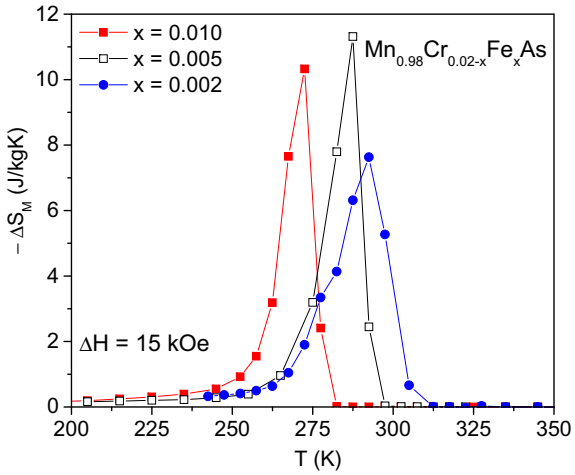

Fig. 6. Magnetic entropy change curves as a function of temperature for a magnetic field of 15 kOe for samples 0.002, 0.005 and 0.010. To avoid artifacts in the entropy change curves, each of the isothermal magnetization curves were measured after heating the sample in zero field up to 390 K and subsequent cooling in zero field down to the measuring temperature.

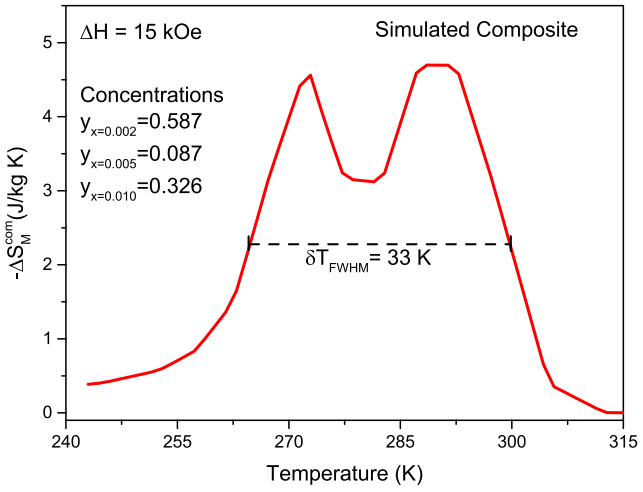

Fig. 7. Simulated magnetic entropy change curve as a function of temperature for simulated composite on applied magnetic field of 15 kOe. Note that the δT_{FWHM} increases from 11 K for a single sample to 33 K for simulated composite.

parts of the Ericsson cycle, i.e., the heat released in low isofield process can be used to regenerate the cycle in the high isofield process, increasing the efficiency of the magnetic refrigeration. We determined the optimum concentration of each compound to form the composite through the method proposed by Smaili and Chahine [27,28]. First, the composite isothermal entropy change ΔS_M^{com} is calculated by

$$\Delta S_M^{com} = \sum_{i=1}^{n} y_i \Delta S_M^i, \tag{2}$$

where n is the number of magnetic materials and y_i its concentrations which $\sum_i^n y_i = 1$. In addition, for an ideal composite, another bond must be considered:

$$\sum_{i=1}^{n} y_i [\Delta S_M^i(T_C^{j+1}) - \Delta S_M^i(T_C^j)] = 0, \tag{3}$$

where j = 1, 2,..., n – 1 and it represents an index of the temperature for the corresponding compound.

Fig. 7 shows the ΔS_M curve for the simulate composite (with δT_{FWHM} = 33 K) which is almost twice larger than that of a single sample (Table 2). Although the ΔS_M^{Max} of the composite has been reduced to 4.7 J/kg K (average value), the Table 2 shows that its RCP is of 162 J/kg, which is considerably increased with respect to the individual samples.

5. Conclusions

In this work, the $Mn_{0.98}Cr_{(0.02-x)}Fe_xAs$ compounds with x = 0.002, 0.005 and 0.010 were produced and the magnetic properties and magnetocaloric effect were investigated. The Fe amount induced a more distorted structure, which emulates a positive pressure effect. This reduction of unit cell volume produced a displacement of T_C to lower temperatures, but it was maintained around the room temperature, as desired for magnetic refrigeration. The transition temperature dependence on pressure rate $\Delta T_C/\Delta P$, indirectly estimated for our magnetic systems, is about ten times the rate measured in $Gd_5Si_2Ge_2$. Since this rate is associated with the barocaloric effect[29], our results point out to the existence of high barocaloric effect in the series $Mn_{0.98}Cr_{(0.02-x)}Fe_xAs$. The ΔS_M was obtained using a measurement protocol which avoided overestimated ΔS_M, which allows to know the realistic values of MCE for Fe-doped MnAs. The ΔS_M^{MAX} values for these compounds are very high, even for 15 kOe applied magnetic field, and they are comparable to the ones observed for those materials considered attractive for magnetic refrigeration. However, a drawback is observed: the δT_{FWHM} of ΔS_M curve is narrow. To overcome this, the ideal compositions of a theoretical composite were determined for obtaining a table-shaped ΔS_M curve. Our results show that the δT_{FWHM} increases from 11 K for a single sample to 33 K for the simulated composite.

Acknowledgements

We acknowledge FAPERJ (Grant Nos. E-26/110.393/2014 and E-16/210.263/2014), CAPES, CNPq (Grant No. 485200/2013-9), FAPESP (Grant No. 2012/03480-0), PROPPI-UFF, MINECO and EU FEDER (project MAT2013-45165-P) and the PAI of the Regional Government of Andalucía for financial support.

References

[1] A. Campos, D.L. Rocco, A.M.G. Carvalho, L. Caron, A.A. Coelho, S. Gama, L.M. Silva, F.C.G. Gandra, A.O. Santos, L.P. Cardoso, P.J. von Ranke, N.A. Oliveira, Ambient pressure colossal magnetocaloric effect tuned by composition in Mn1-xFexAs, Nat. Mater. 5 (2006) 802.
[2] S. Gama, A.A. Coelho, A. de Campos, A.M.G. Carvalho, F.C.G. Gandra, P.J. von Ranke, N.A. de Oliveira, Pressure-induced colossal magnetocaloric effect in MnAs, Phys. Rev. Lett. 93 (2004) 237202.
[3] H. Wada, S. Matsuo, A. Mitsuda, Phys. Rev. B 79 (2009) 092407.
[4] J.N. Gonalves, V.S. Amaral, J.G. Correia, A.M.L. Lopes, Hyperfine interactions in MnAs studied by perturbed angular correlations of rays using the probe and first principles calculations for MnAs and other Mn pnictides, Phys. Rev. B 83 (2011) 104421.
[5] D.L. Rocco, A. de Campos, A.M.G. Carvalho, A.A. Coelho, A.O. dos Santos, L.M. da Silva, S. Gama, M.S. da Luz, L.P. Cardoso, N.A. de Oliveira, J.A. Souza, Influence of chemical doping and hydrostatic pressure on the magnetic properties of $Mn_{1-x}Fe_xAs$ magnetocaloric compounds, Phys. Rev. B 93 (2016) 054431.
[6] M.K. Niranjan, B.R. Sahu, L. Kleinman, Density functional determination of the magnetic state of MnAs, Phys. Rev. B 70 (2004) 180406.
[7] J. Łaewski, P. Piekarz, K. Parlinski, Mechanism of the phase transitions in MnAs, Phys. Rev. B 83 (2011) 054108.
[8] D.L. Rocco, A. de Campos, A.M.G. Carvalho, L. Caron, A.A. Coelho, S. Gama, F.C.G. Gandra, A.O. dos Santos, L.P. Cardoso, P.J. von Ranke, N.A. de Oliveira, Ambient pressure colossal magnetocaloric effect in Mn1 xCuxAs compounds, Appl. Phys. Lett. 90 (2007) 242507.
[9] M. Balli, D. Fruchart, D. Gignoux, C. Dupuis, A. Kedous-Lebouc, R. Zach, Giant magnetocaloric effect in Mn1 x(Ti0.5V0.5)xAs: experiments and calculations, J. Appl. Phys. 103 (2008) 103908.

[10] N.K. Sun, W.B. Cui, D. Li, D.Y. Geng, F. Yang, Z.D. Zhang, Giant room-temperature magnetocaloric effect in Mn1 xCrxAs, Appl. Phys. Lett. 92 (2008) 072507.
[11] B. Kaeswurm, V. Franco, K. Skokov, O. Gutfleisch, Assessment of the magnetocaloric effect in La, Pr(Fe, Si) under cycling, J. Magn. Magn. Mater. 406 (2016) 259–265.
[12] L. Caron, Z. Ou, T. Nguyen, D.C. Thanh, O. Tegus, E. Bruck, On the determination of the magnetic entropy change in materials with first order transitions, J. Magn. Magn. Mater. 321 (21) (2009) 3559–3566.
[13] A.M.G. Carvalho, A. Coelho, P. von Ranke, C. Alves, The isothermal variation of the entropy (Dst) may be miscalculated from magnetization isotherms in some cases: MnAs and Gd5Ge2Si2 compounds as examples, J. Alloys Compd. 509 (8) (2011) 3452–3456.
[14] C.S. Mejia, A.M. Gomes, M.S. Reis, D.L. Rocco, Fe/cr substitution in MnAs compound: increase in the relative cooling power, Appl. Phys. Lett. 98 (2011) 102515.
[15] X. Fu, B. Warot-Fonrose, R. Arras, G. Seine, D. Demaille, M. Eddrief, V. Etgens, V. Serin, In situ observation of ferromagnetic order breaking in MnAs/GaAs(001) and magnetocrystalline anisotropy of MnAs by electron magnetic chiral dichroism, Phys. Rev. B 93 (2016) 104410.
[16] S. Yuce, M. Barrio, B. Emre, E. Stern-Taulats, A. Planes, J.-L. Tamarit, Y. Mudryk, K.A. Gschneidner, V.K. Pecharsky, L. Manosa, Barocaloric effect in the magnetocaloric prototype Gd5Si2Ge2, Appl. Phys. Lett. 101 (2012) 071906.
[17] V. Franco, B.C. Dodrill, C. Radu, Magn. Bus. Technol. 13. (http://www.lakeshore.com/products/Vibrating-Sample-Magnetometer/Pages/MCE.aspx).
[18] D.L. Rocco, J.S. Amaral, J.V. Leitao, V.S. Amaral, M.S. Reis, S. Das, R.P. Fernandes, J.P. Araújo, A.M. Pereira, P.B. Tavares, N.V. Martins, A.A. Coelho, High refrigerant capacity of PrNiCo magnetic compounds exploiting its spin reorientation and magnetic transition over a wide temperature zone, J. Phys. D: Appl. Phys. 42 (5) (2009) 055002.
[19] B.G. Shen, J.R. Sun, F.X. Hu, H.W. Zhang, Z.H. Cheng, Recent progress in exploring magnetocaloric materials, Adv. Mater. 21 (45) (2009) 4545–4564.
[20] R. Zeng, S. Dou, J. Wang, S. Campbell, Large magnetocaloric effect in re-entrant ferromagnet PrMn1.4Ge0.6Ge2, J. Alloys Compd. 509 (7) (2011) L119–L123.
[21] K. Prabahar, D.R. Kumar, M.M. Raja, M. Palit, V. Chandrasekaran, Solidification behaviour and microstructural correlations in magnetocaloric Gd, Si, Ge, Nb alloys, Mater. Sci. Eng.: B 172 (3) (2010) 294–299.
[22] D.L. Rocco, A.A. Coelho, S. Gama, M.d.C. Santos, Dependence of the magnetocaloric effect on the a-site ionic radius in isoelectronic manganites, J. Appl. Phys. 113 (2013) 113907.
[23] R. Das, S. Sarma, A. Perumal, A. Srinivasan, Effect of Co and Cu substitution on the magnetic entropy change in Ni46Mn43Sn11 alloy, J. Appl. Phys. 109 (2011) 07.
[24] D.M.W.D.M. Wang, L. Song, Y.H. Wang, W. Zhang, T.O. Bilige, Magnetocaloric effect in MnFep(0.63)Ge(0.12)Si(0.25)b(x) (x = 0, 0.01, 0.02, 0.03) compounds, Acta Metall. Sin. 47 (3) (2011) 344–348.
[25] R. Caballero-Flores, V. Franco, A. Conde, K.E. Knipling, M.A. Willard, Influence of co and ni addition on the magnetocaloric effect in Fe88 2xCoxNixZr7B4Cu1 soft magnetic amorphous alloys, Appl. Phys. Lett. 96 (2010) 182506.
[26] E.J.R. Plaza, V.S.R. de Sousa, P.J. von Ranke, A.M. Gomes, D.L. Rocco, J.V. Leitao, M.S. Reis, A comparative study of the magnetocaloric effect in RNi2 (R=Nd, Gd, Tb) intermetallic compounds, J. Appl. Phys. 105 (1) (2009) 013903.
[27] A. Smaili, R. Chahine, Composite magnetic refrigerants for an ericsson cycle: new method of selection using a numerical approach, Adv. Cryog. Eng. 42 (1996) 445.
[28] B.P. Alho, P.O. Ribeiro, T.S.T. Alvarenga, A.M.G. Carvalho, P.J. Von Ranke, Magnetocaloric effect in Gd1-yDyyAl2, Fifth IIF-IIR international conference on magnetic refrigeration at room temperature, Grenoble 241 (2012).
[29] T.S.T. Alvaranega, B.P. Alho, E.P. Nobrega, P.O. Ribeiro, A. Caldas, V.S.R. de Sousa, A. Magnus, G. Carvalho, N.A. de Oliveira, P.J. von Ranke, Theoretical investigation on the barocaloric and magnetocaloric properties in the Gd5Si2Ge2 compound, J. Appl. Phys. 116 (2014) 243908.